PHYSICAL REVIEW D VOLUME 50, NUMBER 10 15 NOVEMBER 1994

Axion emission from meson condensates

Takumi Muto
Department of Physics, Kyoto University, Kyoto 606-01, Japan

Toshitaka Tatsumi
*Department of Physics, Kyoto University, Kyoto 606-01, Japan**
and Institut für Theoretische Physik, Universität Heidelberg, D-69120 Heidelberg, Germany

Naoki Iwamoto†
*Department of Physics and Astronomy, The University of Toledo, Toledo, Ohio 43606-3390;**
Yukawa Institute for Theoretical Physics, Kyoto University, Kyoto 606-01, Japan;
and Space Science Laboratory ES65, NASA/Marshall Space Flight Center, Huntsville, Alabama 35812
(Received 9 December 1993)

Axion emission processes in degenerate neutron-star matter in the presence of a condensate of neutral or charged pions or kaons are studied. It is found that the presence of a neutral-pion condensate enhances axion emission over ordinary neutron-star matter as drastically as it enhances neutrino emission. Owing to a quartic temperature dependence, the energy loss due to axion emission in the interior could significantly accelerate the star's thermal evolution for the values of axion parameters that are currently allowed under astrophysical considerations. In addition, it could compete with surface photon radiation for the major part of the star's cooling phase, which may result in a reduced temperature difference between the interior and the surface.

PACS number(s): 97.60.Jd, 14.80.Mz, 21.65.+f

I. INTRODUCTION

The study of elementary processes that contribute to the energy loss of neutron stars is of importance for theoretical understanding of their thermal evolution. A comparison between the theoretical predictions and observations with x-ray satellites in turn gives valuable information about basic particle interactions and the state of matter at high densities and temperatures [1].

The surface temperature of a neutron star (or its upper limit) may be deduced from the measured unpulsed component of the x-ray photon flux by assuming a blackbody spectrum. When the x-ray spectrum can be measured with spectrometers, the surface temperature may also be deduced by fitting the spectrum to a blackbody. The upper limits of the surface temperatures of four sources—3C58 [2], PSR 0531+21 (Crab) [3], RCW 103 [4], and PSR 1929+10 [5]—are consistent with the standard neutrino cooling of ordinary neutron-star matter. The surface temperature of one source, PSR 0656+14 [6], is roughly consistent with or (slightly) lower than the standard cooling scenario, depending on the equation of state. On the other hand, the surface temperatures of two sources, PSR 0833−45 (Vela) [7] and the γ-ray pulsar Geminga [8], are appreciably lower, while that of PSR 1055−52 [9] is (slightly) higher than those predicted by the standard cooling scenario [1,10,11]. One is thus compelled to invoke nonstandard cooling mechanisms at least for PSR 0833−45 and Geminga, and (possibly) for PSR 0656+14, either with the emission of exotic particles, such as axions [12–15], or with exotic matter, such as pion [16–19] or kaon [20–22] condensates, quark matter [23,24], or neutron-star matter with a sufficiently large concentration of protons [25,26] or hyperons [27]. Compared with neutrino emission, thermal emission of exotic particles can enhance the energy loss significantly due to their different couplings to ordinary neutron-star matter, which may result in an increased magnitude and/or different temperature dependence of the energy-loss rate. The presence of exotic matter can modify the kinematical conditions in such a way that the simple β-decay reactions of baryons or quarks may be allowed, thereby enhancing the energy-loss rate significantly compared with the "higher-order" processes, such as the modified Urca process [28] that occurs in ordinary neutron-star matter.

The purpose of the present paper is to look for new energy-loss mechanisms. We do so by combining exotic particles with exotic matter. In particular, we study axion emission processes in meson condensates. We consider axion bremsstrahlung processes involving neutrons, protons, and hyperons in the presence of a condensate of neutral or charged pions or kaons. We find the neutron bremsstrahlung process in the neutral-pion condensate to be of most importance, which, with a quartic temperature dependence ($\propto T^4$), could compete with photon cooling from the surface. In the next section, we calculate the neutron bremsstrahlung rate in a neutral-pion condensate. In Sec. III, we qualitatively discuss

*Present address.
†Electronic address: (internet) iwamoto@uoft02.utoledo.edu

other bremsstrahlung processes including other meson condensates, i.e., proton bremsstrahlung in a neutral-pion condensate, nucleon and hyperon bremsstrahlung in a charged-pion condensate, and neutral- and charged-kaon condensates. In Sec. IV a discussion is given. We compare the axion emission rate with the neutrino emission rate when a neutral-pion condensate is present or absent. We then discuss the implications of axion emission from a neutral-pion condensate in the context of neutron-star cooling. We also comment on the axion emission process involving free pions, which has been considered by other authors. In the Appendix, we note that the momentum supply from the classical pion field arises differently in the matrix elements by examining how the charged and neutral hadronic currents transform under chiral rotation in the different condensate phases. We use the units in which $\hbar = c = k_B = 1$ except in some of the final expressions.

II. AXION EMISSION FROM A NEUTRAL-PION CONDENSATE: NEUTRON BREMSSTRAHLUNG

A. The neutral-pion condensed phase within a chiral-symmetry approach

In this subsection, we first summarize the properties of the neutral-pion (π^0) condensed phase. Within the SU(2)×SU(2) chiral-symmetry model, the neutral-pion condensed phase $|\pi^0\rangle$ is constructed by a chiral rotation of the ground state $|0\rangle$:

$$|\pi^0\rangle = \hat{U}(\pi^0;\phi)|0\rangle \ , \tag{2.1}$$

with

$$\hat{U}(\pi^0;\phi) = \exp\left(i\int d^3r\, A_3^0\phi\right) \ , \tag{2.2}$$

where A_3^μ is the axial-vector current. A classical pion field ϕ is chosen to be of the form $\phi = A\sin k_0 z$, where A and k_0 are the amplitude and the momentum of the condensate, respectively. In this model, the neutral-pion condensate forms a standing wave in one dimension, which is chosen to be in the z direction. The condensate is accompanied by the localization of baryons with a specific spin-isospin order along the z direction, and the baryonic system constitutes the layered structure called the *alternating layer spin* structure in the well-developed ground state [29,30]. Hereafter, we consider the weakly condensed case, where the Fermi surface is little modified from the normal spherical one, and a perturbative treatment with respect to the amplitude A is justified. In this case, the wave functions for neutron quasiparticle states are given by [31]

$$|\tilde{n}(\mathbf{p},\sigma=\pm\tfrac{1}{2})\rangle = |n(\mathbf{p},\sigma=\pm\tfrac{1}{2})\rangle \mp\frac{A\kappa_0}{2}\left(\frac{|n(\mathbf{p}+\mathbf{k}_0,\sigma=\pm\frac{1}{2})\rangle}{\epsilon_N(\mathbf{p}+\mathbf{k}_0)-\epsilon_N(\mathbf{p})}+\frac{|n(\mathbf{p}-\mathbf{k}_0,\sigma=\pm\frac{1}{2})\rangle}{\epsilon_N(\mathbf{p}-\mathbf{k}_0)-\epsilon_N(\mathbf{p})}\right)+O(A^2) \ , \tag{2.3}$$

where σ is the third component of the spin. The proton states are similar. In Eq. (2.3), ϵ_N is the single-particle energy for the nucleon, $\kappa_0 \equiv \tilde{f} f_\pi F_0 k_0 Z_0$ represents the modified pseudovector vertex with $Z_0 = 1/(1+g' F_0^2 \Pi_0)$ and

$$\Pi_0 \equiv 2[U_N(k_0,p_F(p))+U_N(k_0,p_F(n))] +\tfrac{8}{9}(f_{\pi N\Delta}/f_{\pi NN})^2[U_\Delta(k_0,p_F(p))+U_\Delta(k_0,p_F(n))] \ . \tag{2.4}$$

Here, $\tilde{f} \equiv f_{\pi NN}/m_\pi$ is the p-wave pion-nucleon (πNN) coupling constant divided by the pion mass, $f_\pi \cong 93$ MeV is the pion decay constant, and k_0 comes from the πNN pseudovector coupling. In addition, $F_0 \equiv (\Lambda^2 - m_\pi^2)/(\Lambda^2 + k_0^2)$ represents the form factor at the pion-nucleon vertex with the cutoff parameter $\Lambda = 1.2$ GeV, U_N and U_Δ are the Lindhard functions for the nucleon-nucleon particle-hole and Δ-nucleon particle-hole, respectively [32], and $f_{\pi N\Delta}$ ($=\sqrt{72/25}f_{\pi NN}$ in the quark model) is the $\pi N\Delta$ coupling constant. The medium corrections are taken into account through the factor Z_0: (1) excitations of the isobar $\Delta(1232)$, and (2) the short-range correlation in the pion channel, which is simulated by the Landau-Migdal parameter g' within the ring approximation.

It is to be noted that there should be an additional term stemming from Δ excitations in the intermediate states in the wave function (2.3). This term contains propagators of the form $1/[\epsilon_\Delta(\mathbf{p}\pm\mathbf{k}_0)-\epsilon_N(\mathbf{p})]$, where $\epsilon_\Delta(\mathbf{p}\pm\mathbf{k}_0)$ is the single-particle energy of Δ. Approximately, these propagators are of order $1/\delta M_{\Delta N}$ with $\delta M_{\Delta N}$ (=293 MeV) the Δ-N mass difference. As a result, the corresponding phase-space factor $B^{N\Delta}$ in the matrix element for the relevant axion emission processes is smaller than that without the isobars [see (2.15) and (2.16) in Sec. II B] by a typical factor of $O(E_a/\delta M_{\Delta N}) \sim 10^{-4}$–$10^{-5}$, where E_a [$=O(k_BT)$] is the axion energy. Therefore, one may ignore the contributions from the processes involving Δ excitations.

B. Emissivity from neutron bremsstrahlung

We consider the following axion emission processes involving nucleons in the weak neutral-pion condensed phase:

$$\tilde{n}(p) \to \tilde{n}(p') + a(p_a) \tag{2.5a}$$

and

$$\tilde{p}(p) \to \tilde{p}(p') + a(p_a) \ . \tag{2.5b}$$

We denote the four-momenta of the initial and final nucleons and the axion by p, p', and p_a, respectively. For the axion-nucleon coupling we take the interaction Lagrangian density of a pseudovector form [15,33,34]

$$L_{\rm int} = J_h^\mu \partial_\mu a \tag{2.6}$$

with the hadronic current

$$\begin{aligned} J_h^\mu &= [c_p/(f_a/N)]\bar{p}\gamma^\mu\gamma_5 p + [c_n/(f_a/N)]\bar{n}\gamma^\mu\gamma_5 n \\ &\equiv (g_1/m_N)P^\mu + (g_2/m_N)A_3^\mu \ , \end{aligned} \tag{2.7}$$

where c_i ($i = p, n$) is the axion-nucleon coupling, f_a/N the axion decay constant divided by the number of quark flavors, $g_1 \equiv \frac{1}{2}(g_{app} + g_{ann})$, $g_2 \equiv \frac{1}{2}(g_{app} - g_{ann})$ with $g_{aii} \equiv c_i m_N/(f_a/2N)$ the pseudoscalar coupling constant [i.e., the interaction Lagrangian density of the pseudoscalar form is $L = ig_{app}\bar{p}\gamma_5 pa + ig_{ann}\bar{n}\gamma_5 na$] and m_N the nucleon mass. $P^\mu \equiv \frac{1}{2}\bar{N}\gamma^\mu\gamma_5 N$ and $A_3^\mu \equiv \frac{1}{2}\bar{N}\gamma^\mu\gamma_5\tau_3 N$ are the isospin singlet and triplet axial vector currents, respectively, with N the nucleon isodoublet spinor.

For the rest of this section we consider neutron bremsstrahlung (2.5a). We shall consider proton bremsstrahlung (2.5b) in the next section. The emissivity from process (2.5a) is given by

$$\begin{aligned} \epsilon_{an}(\pi^0) = (2\pi/V)[V^3/(2\pi)^9] \\ \times \int d^3p \int d^3p' \int d^3p_a E_a S\delta(E_f - E_i)|M_{an}|^2, \end{aligned} \tag{2.8}$$

where $S = n(\mathbf{p})[1 - n(\mathbf{p}')]$ is the statistical factor, with $n(\mathbf{p})$ the Fermi function and $|M_{an}|^2$ the squared matrix element summed over the initial and final nucleon spin states:

$$\begin{aligned} |M_{an}|^2 &= \sum_{\rm spins}\left|\int d^3r \langle\tilde{n}(p'), a(p_a)|\tilde{H}_{\rm int}|\tilde{n}(p)\rangle\right|^2 \\ &= \sum_{\sigma,\sigma'}\left|\int d^3r \langle\tilde{n}(p',\sigma')|\tilde{J}_h^\mu|\tilde{n}(p,\sigma)\rangle\partial_\mu a\right|^2 , \end{aligned} \tag{2.9}$$

with $\tilde{H}_{\rm int} \equiv \hat{U}(\pi^0)^{-1}H_{\rm int}\hat{U}(\pi^0) = H_{\rm int}$ and $\tilde{J}_h^\mu \equiv \hat{U}(\pi^0)^{-1}J_h^\mu\hat{U}(\pi^0) = J_h^\mu$. Since the hadronic current J_h^μ as well as the Hamiltonian density $H_{\rm int}$ is invariant under the transformation with respect to $\hat{U}(\pi^0)$, there is no *commutator* contribution [16,31], and the momentum of the condensed neutral-pion field k_0 is supplied only through the phase factors $e^{\pm ik_0 z}$ coming from the spatial part of the neutron-quasiparticle wave function (2.3). With the use of a plane wave for the axion $a(x) = (1/\sqrt{2E_aV})e^{ip_a x}$, one obtains

$$|M_{an}|^2 = \sum_{\mu,\nu}(p_a)_\mu(p_a)_\nu M^{\mu\nu}/2E_aV \ . \tag{2.10}$$

In Eq. (2.10),

$$M^{\mu\nu} \equiv \sum_{\sigma,\sigma'}|B_{\sigma'\sigma}|^2 H_{\sigma'\sigma}^{\mu\nu} \ , \tag{2.11}$$

where

$$B_{\sigma'\sigma} = \int d^3r\, \phi_{\sigma'p'}^*(\mathbf{r})\phi_{\sigma p}(\mathbf{r})e^{-i\mathbf{p}_a\mathbf{r}} \tag{2.12}$$

is the phase space factor with $\phi_{\sigma p}(\mathbf{r})$ the spatial part of the wave function (2.3) and

$$H_{\sigma'\sigma}^{\mu\nu} = \langle\chi_{\sigma'}^N|\tilde{J}_h^\mu|\chi_\sigma^N\rangle\langle\chi_{\sigma'}^N|\tilde{J}_h^\nu|\chi_\sigma^N\rangle^* \tag{2.13}$$

is the hadronic tensor. In (2.13), χ_σ^N for $\sigma = \pm\frac{1}{2}$ is the spin part of the wave function. For B_{+-} one obtains

$$\begin{aligned} B_{+-} = \frac{(2\pi)^3}{V}\Bigg[\delta^3(\boldsymbol{\beta}) &+ \frac{A}{2}\left(\frac{1}{\epsilon_N(\mathbf{p}'-\mathbf{k}_0) - \epsilon_N(\mathbf{p}')} - \frac{1}{\epsilon_N(\mathbf{p}+\mathbf{k}_0) - \epsilon_N(\mathbf{p})}\right)\kappa_0\delta^3(\boldsymbol{\beta}+\mathbf{k}_0) \\ &+ \frac{A}{2}\left(\frac{1}{\epsilon_N(\mathbf{p}'+\mathbf{k}_0) - \epsilon_N(\mathbf{p}')} - \frac{1}{\epsilon_N(\mathbf{p}-\mathbf{k}_0) - \epsilon_N(\mathbf{p})}\right)\kappa_0\delta^3(\boldsymbol{\beta}-\mathbf{k}_0)\Bigg] + O(A^2) \ , \end{aligned} \tag{2.14}$$

with $\boldsymbol{\beta} \equiv \mathbf{p} - \mathbf{p}' - \mathbf{p}_a$. The second and the third terms in the square brackets in Eq.(2.14) correspond to the *pole* contributions, which are shown with the diagrams in Fig. 1 [16,31]. The denominators in each term can be simplified with the help of energy conservation $\epsilon_N(\mathbf{p}) = \epsilon_N(\mathbf{p}') + E_a$ and momentum conservation $\boldsymbol{\beta} \pm \mathbf{k}_0 = 0$ by neglecting the axion momentum, since $|\mathbf{p}_a| \sim k_BT/c$. The result is

$$\begin{aligned} \epsilon_N(\mathbf{p}'-\mathbf{k}_0) - \epsilon_N(\mathbf{p}') \sim E_a \ , \\ \epsilon_N(\mathbf{p}+\mathbf{k}_0) - \epsilon_N(\mathbf{p}) \sim -E_a \end{aligned} \tag{2.15a}$$

and

$$\begin{aligned} \epsilon_N(\mathbf{p}'+\mathbf{k}_0) - \epsilon_N(\mathbf{p}') \sim E_a \ , \\ \epsilon_N(\mathbf{p}-\mathbf{k}_0) - \epsilon_N(\mathbf{p}) \sim -E_a \ . \end{aligned} \tag{2.15b}$$

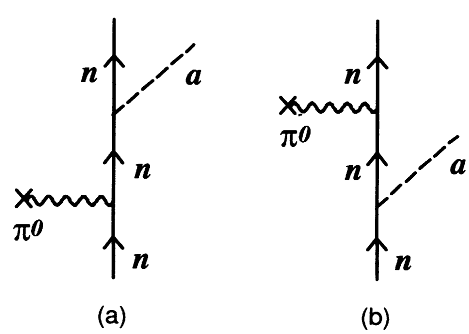

FIG. 1. The lowest-order diagrams for $\tilde{n} \to \tilde{n} + a$. Both diagrams correspond to the pole contribution. The diagrams for $\tilde{p} \to \tilde{p} + a$ are obtained by replacing the neutron lines by proton lines.

By the use of Eqs. (2.15) one obtains

$$B_{+-} = \frac{(2\pi)^3}{V}\left(\delta^3(\boldsymbol{\beta}) + \frac{A\kappa_0}{E_a}[\delta^3(\boldsymbol{\beta}+\mathbf{k}_0) + \delta^3(\boldsymbol{\beta}-\mathbf{k}_0)]\right) + O(A^2) . \tag{2.16a}$$

Other components of the phase-space factor can be obtained in a similar way:

$$B_{-+} = \frac{(2\pi)^3}{V}\left(\delta^3(\boldsymbol{\beta}) - \frac{A\kappa_0}{E_a}[\delta^3(\boldsymbol{\beta}+\mathbf{k}_0) + \delta^3(\boldsymbol{\beta}-\mathbf{k}_0)]\right) + O(A^2) , \tag{2.16b}$$

$$B_{++} = B_{--} = \frac{(2\pi)^3}{V}\delta^3(\boldsymbol{\beta}) + O(A^2) . \tag{2.16c}$$

Next we calculate the hadronic tensor (2.13). In the nonrelativistic limit, P^μ and A_3^μ in (2.7) reduce to

$$P^\mu \to \tfrac{1}{2}\sigma_j\delta^{j\mu} , \quad A_3^\mu \to \tfrac{1}{2}g_A\tau_3\sigma_j\delta^{j\mu} \tag{2.17}$$

for $j = 1,2,3$, respectively, where g_A is the axial vector coupling strength. With the use of (2.17), one obtains the nonzero components of the hadronic tensor

$$\begin{aligned} H_{+-}^{11} &= H_{-+}^{11} = H_{+-}^{22} = H_{-+}^{22} = H_{+-}^{33} = H_{-+}^{33} = (g_1 - \tilde{g}_A g_2)^2/(2m_N)^2 , \\ H_{+-}^{12} &= -H_{-+}^{12} = -H_{+-}^{21} = H_{-+}^{21} = -i(g_1 - \tilde{g}_A g_2)^2/(2m_N)^2 . \end{aligned} \tag{2.18}$$

Here $\tilde{g}_A$ is the axial vector coupling strength with the medium correction renormalized, i.e., $\tilde{g}_A \equiv Z_0 g_A$ [31].

From (2.16) and (2.18), the squared matrix element (2.10) is obtained as

$$|M_{an}|^2 = \frac{(2\pi)^3}{V^2}(g_1 - \tilde{g}_A g_2)^2 \times \frac{A^2\kappa_0^2}{6m_N^2 E_a}[\delta^3(\boldsymbol{\beta}+\mathbf{k}_0) + \delta^3(\boldsymbol{\beta}-\mathbf{k}_0)] + O(A^2) . \tag{2.19}$$

In (2.19), we have averaged the components of the axion momentum as $(p_a^i)^2 = E_a^2/3$ $(i = 1,2,3)$. There is no contribution to the emissivity from the terms that are proportional to $\delta^3(\boldsymbol{\beta})$ in (2.16), since no momentum is supplied from the neutral-pion condensate. After performing the phase-space integration in (2.8), one obtains the final expression for the axion emissivity via neutron bremsstrahlung:

$$\epsilon_{an}(\pi^0) = (\pi/180)(g_1 - \tilde{g}_A g_2)^2 \times (\kappa_0^2 A^2/k_0)(m_n^*/m_n)^2(k_B T)^4 , \tag{2.20}$$

where m_n^* is the effective mass of the neutron. To be specific, let us now employ the numerical values for the physical parameters that have been obtained from the ground-state properties of the neutral-pion condensed phase in neutron-star matter within a chiral-symmetry approach [31]. Near the critical density $\rho_c \sim 2.1\rho_0$, with ρ_0 (=0.17 fm^{-3}) the nuclear matter density, one finds $k_0 \sim 2.1$ fm^{-1}, the proton fraction $Y_p \sim 4\%$, $p_F(n) = 2.1$ fm^{-1}, $p_F(p) = 0.75$ fm^{-1}, so that $\kappa_0 = 0.53$ fm^{-1}, and $Z_0 = 0.43$. Thus, one obtains

$$\epsilon_{an}(\pi^0) \sim 8.0 \times 10^{42}(g_1 - \tilde{g}_A g_2)^2 A^2 \times (m_n^*/m_n)^2 T_9^4 \ \mathrm{erg\,cm^{-3}\,s^{-1}} , \tag{2.21}$$

where T_9 is the temperature in units of 10^9 K.

The quartic temperature dependence of the energy-loss rate may be understood as follows. The squared matrix element (2.9) consists of three factors: the transition amplitude squared, the products of the normalization factors of the wave functions, and the momentum-conserving δ function. The transition amplitude squared is temperature independent, since one power of T from the pseudoscalar axion-nucleon vertex is canceled by an inverse power of T from the propagator for the nonrelativistic nucleon, which is inversely proportional to the axion energy (of order T), while each nucleon line gives rise to no temperature dependence. The normalization of the pseudoscalar (axion) field operator gives rise to an inverse power of T. The momentum-conserving δ function is temperature independent. Thus, the squared matrix element is proportional to an inverse power of T. In addition, the phase-space integrals for both the incoming and outgoing nonrelativistic nucleons yield one power of T each, while the phase-space integral of the axion, which is relativistic, contributes a factor T^3. Furthermore, the energy-loss rate contains the energy of the axion, which yields one power of T, and the energy-conserving δ function contributes a factor T^{-1}. Altogether, the temperature dependence comes out to be T^4.

One may adopt the axion bound from Supernova 1987A to estimate the magnitude of (2.21). From the requirement that the duration of the neutrino signal be no shorter than one-half of the observed duration, together with a simplifying assumption that $g_{ann} = g_{app}$ $(\equiv g_{aNN})$, the upper bound on the axion pseudoscalar coupling constant is [35]

$$g_{aNN} \lesssim (0.3 - 2.6) \times 10^{-10} , \tag{2.22}$$

where the range reflects the theoretical uncertainties. This gives

$$\epsilon_{an}(\pi^0) \lesssim (7.2 \times 10^{20} - 5.4 \times 10^{22})(A^2/0.1) \times (m_n^*/m_n)^2 T_9^4 \ \mathrm{erg\,cm^{-3}\,s^{-1}} . \tag{2.23}$$

One remark is in order. Although the bound from Supernova 1987A, (2.22), is more restrictive than other astrophysical and laboratory constraints, the collisional effects (the Landau-Pomeranchuk effect), which are neglected in deriving (2.22), are likely to relax this bound to some extent [36]. This could possibly *increase* the upper bound on the emissivity (2.23) by an order of magnitude.

III. OTHER BREMSSTRAHLUNG PROCESSES

In this section, we consider other axion emission processes in pion and kaon condensates. Specifically, we consider axion emission from (1) a neutral-pion condensate involving protons (proton bremsstrahlung), (2) a charged-pion condensate, (3) neutral-, and (4) charged-kaon condensates. Using qualitative arguments, we demonstrate that these processes give axion emissivities smaller than that of neutron bremsstrahlung from a neutral-pion condensate.

Let us first consider the axion emission process involving proton quasiparticles $\tilde{p} \to \tilde{p} + a$ (2.5b). In spite of its similarity to the neutron quasiparticle process $\tilde{n} \to \tilde{n} + a$ (2.5a), one finds that the proton process is kinematically suppressed for the following reason. Recall first that the protons are degenerate with the Fermi momentum $p_F(p) \sim 0.75\ \mathrm{fm}^{-1}$, while the static, classical, neutral-pion field can supply the momentum $k_0 \sim 2\ \mathrm{fm}^{-1}$. In order to satisfy energy and momentum conservation simultaneously, the initial and final protons must have momenta at least $p \sim k_0/2$ [$> p_F(p)$]. On the other hand, the number of such suprathermal protons is small. Therefore, the reaction is suppressed due to the presence of a factor $\exp\{-[k_0^2/4 - p_F(p)^2]/2m_N k_B T\} \ll 1$.

Next, we consider axion emission from a charged-pion condensate:

$$\eta \to \zeta + a\ , \tag{3.1a}$$

$$\zeta \to \eta + a\ , \tag{3.1b}$$

where η and ζ are the quasiparticles, which are the superposition of the proton and neutron states [cf. Eqs. (A3) in the Appendix]. Processes (3.1a) and (3.1b) are mediated by the transformed hadronic current (A1). It is to be noted that the momentum supply from the classical pion field takes place through the spatial part of the quasiparticle wave functions (cf. the Appendix), so that a phase factor of the form $\exp(i\mathbf{k}_c \cdot \mathbf{r})$ does not appear explicitly in (A1), which is similar to the case for the neutral-pion condensate. Here $\mathbf{k}_c$ is the momentum of the classical charged-pion field. The calculation of the emissivity from (3.1a) proceeds in the same way as the neutral-pion condensate case, and one obtains

$$\epsilon_{a\eta}(\pi^-) = (\pi^3/126)(1/k_c)[g_2^2 + (g_A^2/3)(2g_1^2 + g_A^2 g_2^2)(k_c/\mu_\pi)^2]\theta^2(m_\eta^*/m_N)(m_\zeta^*/m_N)T^6\ , \tag{3.2}$$

under the condition

$$|p_F(\zeta) - k_c| < p_F(\eta) < |p_F(\zeta) + k_c|\ . \tag{3.3}$$

In (3.2), μ_π is the chemical potential of the classical charged-pion field, $k_c \equiv |\mathbf{k}_c|$, θ is the chiral angle, and m_η^* and m_ζ^* are the effective masses of the quasiparticles η and ζ, respectively. The mixing angle between the neutron and proton states ϕ_c, which is implicit in (3.2), may be approximated as $\phi_c = (g_A k_c/\mu_\pi)\theta + O(\theta^2)$ [37]. The first term in the square brackets of (3.2) is the commutator contribution, while the second term is the pole contribution. The temperature dependence of the emissivity (3.2) is T^6, which is to be compared with the T^4 dependence in the neutral-pion condensate case. The neutron propagator in process (2.5a) is proportional to $1/E_a \sim 1/k_B T$, while the corresponding propagator in the pole contribution in the lowest diagram for (3.1) is proportional to $1/(E_a - \mu_\pi) \sim 1/\mu_\pi$. In addition, the commutator contribution to (3.1) is the same order as the pole contribution, since they are of the same magnitude because of their same temperature dependence. That is, the ratio of the matrix element of the commutator contribution to that of the pole contribution is $O(k_c/\mu_\pi) \sim 1$. Thus, the ratio of the squared matrix elements for (3.1) and (2.5a) is

$$|M(\eta \to \zeta + a)|^2/|M(\tilde{n} \to \tilde{n} + a)|^2 \sim (k_B T/\mu_\pi)^2 \ll 1\ . \tag{3.4}$$

Therefore, one expects the ratio of the energy-loss rates from these processes to be of the same order:

$$\epsilon_{a\eta}(\pi^-)/\epsilon_{an}(\pi^0) \sim (k_B T/\mu_\pi)^2 \ll 1\ , \tag{3.5}$$

apart from the different phase-space factors (for the proton and the neutron), which are unlikely to compensate the small factor $(k_B T/\mu_\pi)^2$. Furthermore, soon after the onset of the charged-pion condensate, the ground state consists only of η particles (within the one-Fermi-sea approximation) [37], where the kinematical condition (3.3) is not satisfied. For these reasons, we conclude that axion emission is not as important in a charged-pion condensate as in a neutral-pion condensate.

We now speculate on the axion emission processes from kaon condensations. Here we briefly remark on the ground-state properties of the kaon condensed phase. The possibility of kaon condensation was pointed out by Kaplan and Nelson [38]. In recent works by two of us, it has been shown that the weak interactions play an important role in the realization of the kaon condensate in stable neutron matter [30,39–41]. The chemical equilibrium is attained via the weak process, $n \leftrightarrow p + K^-$, which leads to the appearance of protons. The proton fraction is found to increase drastically once the condensed kaons appear, due to larger s-wave KN attractive interactions for protons than for neutrons. As a result, the protons and neutrons, which provide two Fermi seas independently, come into play in the condensed phase virtually equally.

Based on these aspects of the negatively charged kaon condensed phase, we consider the following axion emission process from a charged-kaon condensate:

$$\eta_K \to \zeta_K + a \ , \tag{3.6a}$$

$$\zeta_K \to \eta_K + a \ , \tag{3.6b}$$

where η_K and ζ_K particles are superpositions of the neutron and proton states:

$$|\eta_K(\mathbf{p},\sigma=\pm\tfrac{1}{2})\rangle = u|n(\mathbf{p},\sigma=\pm\tfrac{1}{2})\rangle + v|p(\mathbf{p},\sigma=\pm\tfrac{1}{2})\rangle, \tag{3.7a}$$

$$|\zeta_K(\mathbf{p},\sigma=\pm\tfrac{1}{2})\rangle = u^*|p(\mathbf{p},\sigma=\pm\tfrac{1}{2})\rangle - v^*|n(\mathbf{p},\sigma=\pm\tfrac{1}{2})\rangle. \tag{3.7b}$$

Note that $u = 1 + O(G_F^2)$ and $v = O(G_F)$ with G_F the Fermi constant, because the protons, neutrons, and condensed kaons couple only through the weak interactions. The transformed hadronic current is given by

$$\begin{aligned}\tilde{J}_h^\mu &= \hat{U}^{-1}(K^-;\mu_K,\theta_K)J_h^\mu\hat{U}(K^-;\mu_K,\theta_K)\\ &= (g_1/m_N)P^\mu + (g_2/m_N)[A_3^\mu + \tfrac{1}{4}(\cos\theta_K - 1)\\ &\quad\times(A_3^\mu + \sqrt{3}A_8^\mu) - \tfrac{1}{2}V_5^\mu \sin\theta_K]\end{aligned} \tag{3.8}$$

with a unitary operator generating the charged-kaon condensed state

$$\hat{U}(K^-;\mu_K,\theta_K) \equiv \exp(i\mu_K tQ)\ \exp(i\theta_K Q_4^5)\ , \tag{3.9}$$

where $Q \equiv V_3^0 + V_8^0/\sqrt{3}$ is the electromagnetic charge operator, and μ_K and θ_K are the chemical potential and the chiral angle, respectively, of the classical charged-kaon field. From Eqs. (3.7) and (3.8), we can see that the commutator term [$\propto V_5^\mu \sin\theta_K$ in (3.8)] does not contribute to the matrix elements within the nonrelativistic approximation and that only the pole terms from the flavor-conserving currents in (3.8) contribute. However, the latter are mediated by the weak interaction, $n \to p + K^-$, so that the emission rate is expected to be much smaller than that from (2.5). In addition, the kinematical condition is not satisfied at the aNN vertex because the classical kaon field is of the s-wave type (with the momentum $\mathbf{p}_K = 0$), which is in contrast with the charged-pion condensate case. Therefore, the process (3.6) is hardly important compared with other processes.

At a certain density over the threshold of the s-wave negatively charged-kaon condensation, the condensate becomes of the p-wave type (with $|\mathbf{p}_K| \neq 0$), where hyperon (Y) excitations appear via the KNY strong interactions [30,39–41]. The generator of the p-wave kaon condensation has a form that is the extension of (3.9) to a p wave:

$$\begin{aligned}\hat{U}(K^-;\mu_K,\mathbf{p}_K,\theta_K) \equiv &\exp(i\mu_K tQ)\\ &\times\exp\left(i\int d^3r\,\mathbf{p}_K\cdot\mathbf{r}V_V^0\right)\\ &\times\exp(i\theta_K Q_4^5)\end{aligned} \tag{3.10}$$

with the V-spin charge density $V_V^0 \equiv (V_3^0 + \sqrt{3}V_8^0)/2$. Thereby the transformed hadronic current results in the same form as (3.8). Thus, a phase factor of the form $\exp(i\mathbf{p}_K\cdot\mathbf{r})$ does not appear from the transformed hadronic current either. On the other hand, baryons are composed of quasiparticles as superpositions of the nucleon and hyperon states. The neutron couples to the Σ^-, while the proton couples to the Λ and Σ^0, respectively. For example,

$$\begin{aligned}|\tilde{n}(\mathbf{p},\,\sigma=\pm\tfrac{1}{2})\rangle = &\cos\phi_K|n(\mathbf{p}-\mathbf{p}_K/2,\,\sigma=\pm\tfrac{1}{2})\rangle\\ &\pm i\,\sin\phi_K|\Sigma^-(\mathbf{p}-\mathbf{p}_k/2,\,\sigma=\pm\tfrac{1}{2})\rangle\ ,\end{aligned} \tag{3.11a}$$

$$\begin{aligned}|\tilde{\Sigma}^-(\mathbf{p},\sigma=\pm\tfrac{1}{2})\rangle = &\cos\phi_K|\Sigma^-(\mathbf{p}+\mathbf{p}_K/2,\sigma=\pm\tfrac{1}{2})\rangle\\ &\pm i\,\sin\phi_K|n(\mathbf{p}+\mathbf{p}_K/2,\,\sigma=\pm\tfrac{1}{2})\rangle\ ,\end{aligned} \tag{3.11b}$$

and $|\tilde{p}\rangle$, $|\tilde{\Lambda}\rangle$, and $|\tilde{\Sigma}^0\rangle$ take similar forms. In (3.11), ϕ_K is the mixing angle between the nucleon and the hyperon through the p-wave KNY coupling (which has a feature $\phi_K \to 0$ as $\mathbf{p}_K \to 0$). Then, the transition from $|\tilde{n}\rangle$ to $|\tilde{\Sigma}^-\rangle$ (and from $|\tilde{p}\rangle$ to $|\tilde{\Lambda}\rangle$ or $|\tilde{\Sigma}^0\rangle$) and vice versa are possible via both the commutator and pole terms in (3.8), and the momentum is supplied through the phase shift in the spatial wave functions between the $|\tilde{n}\rangle$ and $|\tilde{\Sigma}^-\rangle$ states (and between the $|\tilde{p}\rangle$ and $|\tilde{\Lambda}\rangle$ or $|\tilde{\Sigma}^0\rangle$ states). These cases are similar to that of the charged-pion condensate and the resultant emissivity has a T^6 temperature dependence. Nevertheless, the ground state is likely to consist only of $|\tilde{n}\rangle$ and $|\tilde{p}\rangle$ states [30,41] because the $|\tilde{\Sigma}^-\rangle$ and the $|\tilde{\Lambda}\rangle$ or $|\tilde{\Sigma}^0\rangle$ states have larger single-particle energies than those for the $|\tilde{n}\rangle$ and $|\tilde{p}\rangle$ states. As a result, these processes are likely to be kinematically suppressed. Thus, axion emission processes in a p-wave kaon condensate are expected to play a minor role as compared with the case of a neutral-pion condensate.

When a neutral-kaon condensate is present [42], one might be interested in the processes

$$\tilde{n} \to \tilde{n} + a\ , \tag{3.12a}$$

$$\tilde{p} \to \tilde{p} + a\ . \tag{3.12b}$$

Here, $\tilde{n}$ and $\tilde{p}$ represent quasiparticles. On the other hand, since the neutral-kaon condensate occurs in the s-wave state on a macroscopic (or classical) scale, no momentum supply is available from the condensate. In addition, the reactions $n \leftrightarrow n + K^0$ and $p \leftrightarrow p + K^0$ lead to the chemical equilibrium condition for the chemical potential of the neutral-kaon $\mu_{K^0} = 0$. This means that no energy supply is available from the condensate either. Therefore, reactions (3.12a) and (3.12b) are "classically" forbidden. For this reason, these reactions must proceed through thermal excitations in the condensate. But, since such reactions are of higher order, we expect the rate to be small. We might add that the nature of the neutral-kaon condensation itself has not been studied in detail and, therefore, is not well known.

IV. DISCUSSION

It is instructive to compare axion emission with neutrino emission in the two cases when a pion condensate is present or absent. In the absence of a pion condensate, the major axion emission mechanism is nucleon-nucleon bremsstrahlung [12–14], while neutrinos are emitted via the modified Urca process [28]. The ratio of the emissivities through these two mechanisms is given by

$$\epsilon_{ann}/\epsilon_{\text{mod-Urca}} \sim 8.8 \times 10^{16}(g_{ann}^2/\hbar c)(m_n/m_n^*)(m_p/m_p^*)(\rho/\rho_0)^{-1/3}T_9^{-2} \,. \tag{4.1}$$

The neutron and proton effective masses are denoted by m_n^* and m_p^*, respectively. In addition, only the neutron-neutron bremsstrahlung rate is used for the axion emissivity. The inclusion of proton-proton and neutron-proton bremsstrahlung increases the rate typically by a factor of 2–3 for $g_{app} = 0$ and $g_{ann} \neq 0$ and 3–7 for $g_{app} = g_{ann}$ for the range of the mass density $1 \leq \rho/\rho_0 \leq 10$ [14]. In the presence of a neutral-pion condensate, one may use the rate calculated in the present paper for axion emission, while the Urca process becomes the major neutrino emission mechanism [31]. Then, the ratio of the axion emission rate to the neutrino emission rate is

$$\epsilon_{an}(\pi^0)/\epsilon_{\text{Urca}}(\pi^0) \sim 4.8 \times 10^{16}(g_{aNN}^2/\hbar c)(m_n^*/m_n)(m_p/m_p^*)T_9^{-2} \,. \tag{4.2}$$

Here, we have set $g_{app} = g_{ann} \equiv g_{aNN}$ for simplicity. By comparing (4.1) and (4.2), one finds that the ratio of the axion emission rate to the neutrino emission rate in the presence of a neutral-pion condensate is roughly the same as the ratio in the absence of a pion condensate [43].

This is not surprising for the following reason. Let us recall that energy conservation and momentum conservation give two independent constraints on the momenta of the particles involved in the reaction if some of these particles are nonrelativistic. Another important constraint comes from phase space due to the Pauli principle: The momenta of the degenerate fermions involved in the reaction must lie close to their respective Fermi surfaces for the reaction to occur at an appreciable rate. For ordinary neutron-star matter, the composition of the degenerate fermions combined with these constraints do not permit the simple neutron β decay reactions to proceed, and the modified Urca process with a degenerate bystander nucleon that takes up excess momentum becomes the lowest-order process to be allowed [44]. The situation is somewhat similar to a nucleon bremsstrahlung. A single nucleon cannot emit a neutrino pair via the bremsstrahlung, since such a process cannot satisfy the energy and momentum conservation laws simultaneously [45]. A nucleon-nucleon bremsstrahlung (again with a bystander nucleon) becomes the lowest-order process [28]. The presence of pion condensates changes the mechanism of neutrino emission drastically—since both the charged- and neutral-pion condensates may supply or absorb momentum, the simple β decay reactions [16–18] and the neutrino pair bremsstrahlung by a single nucleon [31] are, respectively, kinematically allowed. This means that the number of degenerate fermions involved in the reactions is smaller, and thus the reactions suffer less Pauli blocking, resulting in larger neutrino emission rates. However, the same is true for axion emission. Therefore, the ratio of the neutrino and axion emission rates is not changed significantly whether or not pions are present. Roughly speaking, the only major difference between axion emission and neutrino emission is that while an axion is emitted singly by a nucleon, the (anti)neutrino is emitted in the form of a lepton pair (an electron and an electron-type antineutrino) by a nucleon (accompanied by the change in nucleon isosopin). The rest, either nucleon-nucleon collision or nucleon-pion condensate interactions, is essentially the same.

Let us now discuss the implications of the axion emission mechanism considered in the present paper for neutron star cooling. The quartic temperature dependence of the axion emissivity in the neutral-pion condensate implies that this cooling mechanism persists at low temperatures. For ordinary neutron-star matter, the conventional neutrino cooling mechanisms, such as the modified Urca process, nucleon bremsstrahlung, and electron bremsstrahlung in the crust, all depend on the temperature with higher powers (T^8, T^8, and T^6, respectively) [46]. Here, T is the temperature of the interior. Photon cooling from the surface eventually dominates at later stages with the temperature dependence of T_e^4 with T_e the temperature of the surface. Here, the temperature of the interior T is related to the temperature of the surface T_e through the thermal properties of the crust (thickness, composition, and radiative and conductive opacities, etc.), which are determined by such factors as the equation of state, the magnetic field strength, and the mass of the neutron star. Typically, $T \sim 10^2 T_e$ at $T_e \sim 10^6$ K [46–48]. The situation is considerably different in the presence of a pion condensate [16–18]. As mentioned in the preceding paragraph, the simple β decay of nucleon quasiparticles is kinematically allowed in the presence of a charged-pion condensate so that neutrino emission is significantly enhanced. Furthermore, the temperature dependence of the neutrino emission rate goes as T^6, such that the neutrino emission persists at lower temperatures. The picture may be further changed with axion cooling in the presence of a neutral-pion condensate. The temperature dependence of the energy loss rate is now the same—T^4 in the interior and T_e^4 on the surface. Therefore, if the axion cooling in the interior exceeds the photon cooling from the surface, the former may be dominant throughout the entire cooling stage. The photon cooling no longer has the advantage of having milder temperature dependence compared with the internal cooling mechanisms. In order to illustrate this point, let us compare the blackbody surface photon emission rate by a neutron star of radius R (and volume $V = 4\pi R^3/3$ with σ the Stefan-Boltzmann constant),

$$\epsilon_\gamma = 4\pi R^2 \sigma T_e^4/V = 1.7 \times 10^{26} (R/10 \text{ km})^{-1} T_{e9}^4 \text{ erg cm}^{-3}\text{ s}^{-1} , \quad (4.3)$$

with the axion emission rate (2.21), assuming that $g_{app} = g_{ann} \equiv g_{aNN}$ for simplicity together with the bound (2.22):

$$\epsilon_{an}(\pi^0)/\epsilon_\gamma = 4.7 \times 10^{16} (g_{aNN}^2/\hbar c) A^2 (m_n^*/m_n)^2 (R/10 \text{ km})(T/T_e)^4 \lesssim (4 \times 10^2 - 3 \times 10^4)(A^2/0.1)(m_n^*/m_n)^2 (R/10 \text{ km})(T_9/T_{e7})^4 . \quad (4.4)$$

Here $T_9 \equiv T/10^9$ K and $T_{e7} \equiv T_e/10^7$ K. This clearly demonstrates the importance of axion emission compared with surface photon emission. The consequence of this enhanced cooling due to axion emission would be a reduced temperature difference between the interior and the surface. A numerical evolutionary calculation should reveal the details of the thermal history of such a neutron star.

For ordinary neutron-star matter, the energy-loss rates due to axion emission and neutrino emission have been compared in order to obtain bounds on the axion-nucleon coupling constants [12–14]. Similar comparison can be made in the presence of a pion condensate in order to obtain axion bounds. One expects such bounds in the presence of a pion condensate to be as good as (i.e., of the same order of magnitude as), but not significantly better than, those in the absence of a pion condensate. The reasons is that, while axion emission is enhanced (for a given coupling strength) by the presence of a pion condensate, neutrino emission is enhanced as well by roughly the same amount. In this connection, it is appropriate to mention a recent work by Turner [49], in which he calculates the axion emission rate from *nondegenerate* neutron-star matter in the presence of free charged pions. He finds that axion emission is enhanced with pions compared to the case without pions. He then concludes that a better bound on the axion-nucleon coupling constant would result from the observed neutrino events of Supernova 1987A. As is apparent from the previous discussion, this does not seem consistent. First, if pions are abundant, neutrino emission is enhanced as well. Therefore, the enhanced axion emission should be compared to the enhanced neutrino emission when the pions are present. Second, if pions are abundant, one must check whether the observed neutrino pulse is consistent with the collapse model and the calculated duration of the neutrino pulse. This is because the presence of pions as abundant as the nucleons themselves would soften the equation of state and may not lead to the core bounce, which is essential to supernova explosion. In addition, the presence of free pions enhances the production as well as the absorption of the neutrinos, such that it will alter the neutrino mean free path significantly and thus the duration of the neutrino pulse [17].

Finally, let us make a general remark on the implications of new rapid cooling mechanisms, such as those studied in this paper, on the current observations. As mentioned in the Introduction, four sources 3C58, PSR 0531+21 (Crab), RCW 103, and PSR 1929+10 give only upper limits to the surface temperatures. Therefore, these data neither contradict nor confirm the standard cooling scenario, i.e., the neutrino cooling of ordinary neutron-star matter. The data for PSR 0833−45 (Vela) and Geminga do contradict the standard cooling scenario. Even if the four sources, such as 3C58, etc., turn out to have surface temperatures that are current upper limits, one does not have to explain all the data in one type of matter. The variation in mass, for example, may result in some having ordinary neutron-star matter and others having a pion condensate or quark matter in their cores. Therefore, an attempt to finding a possible explanation for rapid cooling does not adversely affect the interpretation of the data that are currently consistent with the standard scenario. Furthermore, the purpose of finding new rapid-cooling mechanisms is not limited to explaining the data for PSR 0833−45 and Geminga. There are several supernova remnants, such as SN 1680 (Cas A) [50,51], SN 1572 (Tycho) [52], and SN 1006 [51,53], in which no neutron stars have been detected with the temperature upper limits significantly below those predicted by the standard scenario for their ages. Among many possibilities, one obvious possibility is that these supernova events did not produce neutron stars. Another possibility is that there are neutron stars in some of them but they are too cool to be detected with the current instruments.

ACKNOWLEDGMENTS

We wish to thank Professor R. Tamagaki for encouragement. T.T. would like to thank Professor J Hüfner for hospitality during his stay at Heidelberg. N.I. wishes to thank Dr. R. Cornett and Dr. M. C. Weisskopf for hospitality during his visit to Huntsville, and Professor R. T. Deck and Professor C. G. Montgomery for comments on the manuscript. This material is based upon work supported in part by the National Science Foundation through the Theoretical Physics Program under Grant No. PHY-90-08475. N.I. also wishes to acknowledge additional support from Hughes STX Corporation under Contract No. NAS8-39204 and from the College of Arts and Sciences at the University of Toledo through the Faculty Development Fund.

APPENDIX: CHIRAL ROTATION OF THE HADRONIC CURRENTS AND THE MOMENTUM SUPPLY FROM THE PION CONDENSATE

The axion emission processes (2.5) are mediated by the hadronic current J_h^μ (2.7). In this appendix we remark on the relation between the properties of the hadronic currents, such as (2.7), under chiral rotation and how the momentum is supplied from the classical pion field within the framework of chiral symmetry.

In the neutral pion condensed phase, the (flavor-conserving isospin) hadronic current (2.7) is invariant under the chiral rotation with respect to the unitary operator $\hat{U}(\pi^0)$ (2.2) as seen in Sec. II B. In the charged-pion condensed phase, on the other hand, the current transforms as

$$\hat{U}(\pi^c;\mu_\pi,k_c,\theta)^{-1}J_h^\mu\hat{U}(\pi^c;\mu_\pi,k_c,\theta) = (g_1/m_N)P^\mu + (g_2/m_N)(A_3^\mu\cos\theta - V_2^\mu\sin\theta)\ . \tag{A1}$$

Here, $\hat{U}(\pi^c;\mu_\pi,k_c,\theta)$ is the unitary operator, which generates the charged-pion condensed phase with a macroscopic charged-pion field of chemical potential μ_π, momentum k_c, and the chiral angle θ [37,54]:

$$\hat{U}(\pi^c;\mu_\pi,k_c,\theta) = \exp\left(i\int d^3r\,\chi V_3^0\right)\exp(iQ_1^5\theta) \tag{A2}$$

with $\chi \equiv \mathbf{k}_c\cdot\mathbf{r} - \mu_\pi t$. Thus, in either case, the hadronic current does not acquire a phase factor of the form $\exp(i\mathbf{k}\cdot\mathbf{r})$ under the transformation with respect to $\hat{U}(\pi^0)$ or $\hat{U}(\pi^c)$. The situation is similar for the neutral (flavor-conserving isospin) current, which is relevant for the nucleon bremsstrahlung processes [31]. In con-

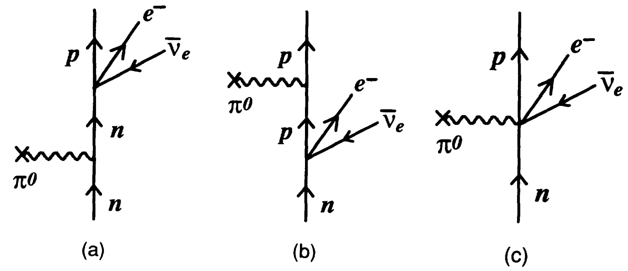

FIG. 2. The lowest-order diagrams for $\tilde{n}\to\tilde{p}+e^-+\bar{\nu}_e$. Diagrams (a) and (b) correspond to the pole contribution and (c) to the commutator contribution. The diagrams for the inverse process $\tilde{p}+e^-\to\tilde{n}+\nu_e$ are obtained by interchanging the neutron and proton lines, replacing the outgoing electron line by an incoming electron line, and replacing the antineutrino line by a neutrino line.

TABLE I. The properties of the (flavor-conserving and flavor-changing) hadronic isospin currents under the chiral transformations and the patterns of momentum supply from the classical (neutral and charged) pion fields. The sources of momentum supply are indicated whether it is from the wave function, from the chirally transformed current, or from both.

		Flavor-conserving isospin current $J_h^\mu = (g_1/m_N)P^\mu + (g_2/m_N)A_3^\mu$	Flavor-changing isospin current $J_{h,1+i2}^\mu = V_1^\mu + A_1^\mu + i(V_2^\mu + A_2^\mu)$
Neutral-pion condensate	Processes	$\tilde{n}\to\tilde{n}+a$, $\tilde{p}\to\tilde{p}+a$	$\tilde{n}\to\tilde{p}+e^-+\bar{\nu}_e$, $\tilde{p}+e^-\to\tilde{n}+\nu_e$
	Lowest-order diagrams	See Figs. 1(a) and 1(b).	See Figs. 2(a)–2(c).
	Transformation	$\tilde{J}_h^\mu \equiv \hat{U}(\pi^0)^{-1}J_h^\mu\hat{U}(\pi^0) = J_h^\mu$	$\tilde{J}_{h,1+i2}^\mu \equiv \hat{U}(\pi^0)^{-1}J_{h,1+i2}^\mu\hat{U}(\pi^0) = e^{i\phi}[V_1^\mu + A_1^\mu + i(V_2^\mu + A_2^\mu)]$
	Momentum supply	Wave function	Current and wave function
	References	Present work (Sec. II)	[31]
Charged-pion condensate	Processes	$\eta\to\zeta+a$, $\zeta\to\eta+a$	$\eta\to\eta+e^-+\bar{\nu}_e$ $\zeta\to\zeta+e^-+\bar{\nu}_e$, $\eta+e^-\to\eta+\nu_e$ $\zeta+e^-\to\zeta+\nu_e$
	Lowest-order diagrams	See Figs. 3(a)–3(c).	See Figs. 4(a) and 4(b).
	Transformation	$\tilde{J}_h^\mu \equiv \hat{U}(\pi^c)^{-1}J_h^\mu\hat{U}(\pi^c) = (g_1/m_N)P^\mu + (g_2/m_N)(A_3^\mu\cos\theta - V_2^\mu\sin\theta)$	$\tilde{J}_{h,1+i2}^\mu \equiv \hat{U}(\pi^c)^{-1}J_{h,1+i2}^\mu\hat{U}(\pi^c) = e^{i\chi}\{V_1^\mu + A_1^\mu + i[(V_2^\mu + A_2^\mu)\cos\theta + (V_3^\mu + A_3^\mu)\sin\theta]\}$
	Momentum supply	Wave function	Current
	References	Present work (Sec. III)	[16–19]

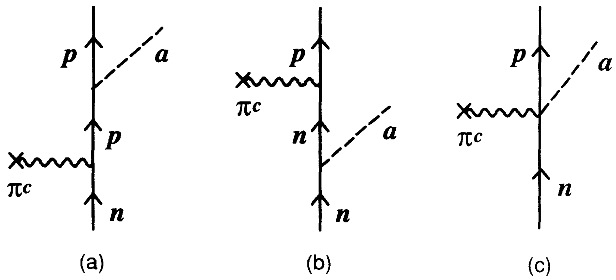

FIG. 3. The lowest-order diagrams for $\eta \to \zeta + a$. The neutron and proton states of the η and ζ particles, respectively, are explicitly shown. Diagrams (a) and (b) correspond to the pole contribution and (c) to the commutator contribution. The diagrams for $\zeta \to \eta + a$ are obtained by interchanging the neutron and proton lines.

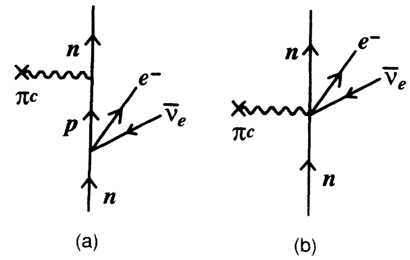

FIG. 4. The lowest-order diagrams for $\eta \to \eta + e^- + \bar{\nu}_e$. Diagrams (a) and (b) correspond to the pole contribution and the commutator contribution, respectively. The diagrams for the inverse process $\eta + e^- \to \eta + \nu_e$ are obtained by interchanging the pion-nucleon and weak vertices, replacing the outgoing electron line by an incoming electron line, and replacing the antineutrino line by a neutrino line. The diagrams for the corresponding process involving the ζ particle (and its inverse) are obtained from the diagrams for the η particle processes by interchanging the neutron and proton lines.

trast, the hadronic charged (or flavor-changing isospin) current $J^\mu_{h,1+i2} \equiv V^\mu_1 + A^\mu_1 + i(V^\mu_2 + A^\mu_2)$, which is relevant for the Urca process, acquires a phase factor of the form $\exp(i\mathbf{k}\cdot\mathbf{r})$ under both types of chiral transformations with respect to $\hat{U}(\pi^0)$ and $\hat{U}(\pi^c)$ [16,18,31]. Physically, this phase factor expresses the momentum supply from the classical pion field in the neutrino emission process. As for the hadronic current (2.7), such a phase factor appears not from the chiral transformation, as noted above, but through the spatial part of the nucleon wave functions: In the case of the neutral-pion condensate, the momentum supply from the classical neutral-pion field may be seen in the phase factor in the wave function (2.3). In the case of the charged-pion condensate, on the other hand, the participating particles for the axion emission process are quasiparticles η and ζ, which are the superpositions of the proton and neutron states:

$$|\eta(\mathbf{p}, \sigma = \pm\tfrac{1}{2})\rangle = \cos\phi_c |n(\mathbf{p} + \mathbf{k}_c/2, \sigma = \pm\tfrac{1}{2})\rangle \mp i \sin\phi_c |p(\mathbf{p} + \mathbf{k}_c/2, \sigma = \pm\tfrac{1}{2})\rangle , \quad \text{(A3a)}$$

$$|\zeta(\mathbf{p}, \sigma = \pm\tfrac{1}{2})\rangle = \cos\phi_c |p(\mathbf{p} - \mathbf{k}_c/2, \sigma = \pm\tfrac{1}{2})\rangle \mp i \sin\phi_c |n(\mathbf{p} - \mathbf{k}_c/2, \sigma = \pm\tfrac{1}{2})\rangle , \quad \text{(A3b)}$$

where ϕ_c is the mixing angle given by $\phi_c = (g_A k_c/\mu_\pi)\theta + O(\theta^2)$ in the weak condensate. Note that fields η and ζ tend to n and p, respectively, as $\phi_c \to 0$ (or $\theta \to 0$). Then the axion emission process is written as

$$\eta \to \zeta + a , \quad \text{(A4a)}$$

$$\zeta \to \eta + a . \quad \text{(A4b)}$$

There is a shift in momentum by $\mathbf{k}_c$ between the wave functions of quasiparticles η and ζ, which expresses the momentum supply from the pion field. It is to be noted that a contact term of the form $V^\mu_2 \sin\theta$ appears in (A1) for this process (a *commutator* contribution), which is inherent in the chiral-symmetry approach. In Table I we summarize the properties of the hadronic currents under the chiral transformations as well as the patterns of the momentum supply from the classical pion fields for the relevant processes.

[1] S. Tsuruta, Comments Astrophys. **11**, 151 (1986).
[2] R. H. Becker, D. J. Helfand, and A. E. Szymkowiak, Astrophys. J. **255**, 557 (1982).
[3] F. R. Harnden, Jr. and F. D. Seward, Astrophys. J. **283**, 279 (1984).
[4] W. Becker, J. Trümper, G. Hasinger, and B. Aschenbach, in *Isolated Pulsars: Proceedings of the Los Alamos Workshop*, Taos, New Mexico, 1992, edited by K. A. Van Riper, R. Epstein, and C. Ho (Cambridge University Press, Cambridge, U.K., 1993), p. 116.
[5] A. Alpar, W. Brinkmann, Ü. Kiziloglu, H. Ögelman, and D. Pines, Astron. Astrophys. **177**, 101 (1987).
[6] J. P. Finley, H. Ögelman, and U. Kiziloglu, Astrophys. J. Lett. **394**, L21 (1992).
[7] H. Ögelman, J. P. Finley, and H. U. Zimmermann, Nature (London) **361**, 136 (1993).
[8] J. P. Halpern and S. S. Holt, Nature (London) **357**, 222 (1992); J. P. Halpern and M. Ruderman, Astrophys. J. **415**, 286 (1993).
[9] W. Brinkmann and H. Ögelman, Astron. Astrophys. **182**, 71 (1987).
[10] K. Nomoto and S. Tsuruta, Astrophys. J. **312**, 711 (1987).
[11] It is to be noted that the low-energy imaging telescopes

combined with various filters on board EXOSAT and the Position Sensitive Proportional Counter on board ROSAT give spectral information for the x-ray photons. The data for the positively detected point sources PSR 1055−52 (EXOSAT; Ref. [9]) and PSR 0656+14 (ROSAT; Ref. [6]—with or without the possible presence of a helium atmosphere) are consistent with the blackbody spectrum. On the other hand, the spectra of PSR 0833−45 (ROSAT; Ref. [7]) and Geminga (ROSAT; Ref. [8]) show a soft blackbody component with a high-energy excess. Since the soft component of the x-ray flux from these sources constitutes the major part, the x rays are thought to be coming from the surface.

[12] N. Iwamoto, Phys. Rev. Lett. **53**, 1198 (1984).

[13] N. Iwamoto, Phys. Rev. D **39**, 2120 (1989).

[14] N. Iwamoto (unpublished).

[15] For reviews, see, e.g., M. S. Turner, Phys. Rep. **197**, 67 (1990); G. G. Raffelt, *ibid.* **198**, 1 (1990).

[16] O. Maxwell, G. E. Brown, D. K. Campbell, R. F. Dashen, and J. T. Manassah, Astrophys. J. **216**, 77 (1977).

[17] R. F. Sawyer and A. Soni, Astrophys. J. **216**, 73 (1977); T. Tatsumi, Prog. Theor. Phys. Suppl. **91**, 299 (1987).

[18] T. Tatsumi, Prog. Theor. Phys. **69**, 1137 (1983).

[19] H. Umeda, K. Nomoto, S. Tsuruta, T. Muto, and T. Tatsumi, Astrophys. J. **431**, 309 (1994).

[20] G. E. Brown, K. Kubodera, D. Page, and P. Pizzochero, Phys. Rev. D **37**, 2042 (1988).

[21] T. Tatsumi, Prog. Theor. Phys. **80**, 22 (1988).

[22] D. Page and E. Baron, Astrophys. J. Lett. **354**, 17 (1990).

[23] N. Iwamoto, Phys. Rev. Lett. **44**, 1637 (1980).

[24] N. Iwamoto, Ann. Phys. (N.Y.) **141**, 1 (1982).

[25] J. M. Lattimer, C. J. Pethick, M. Prakash, and P. Haensel, Phys. Rev. Lett. **66**, 2701 (1991). See also J. Boguta, Phys. Lett. **106B**, 255 (1981).

[26] D. Page and J. H. Applegate, Astrophys. J. Lett. **394**, L17 (1992).

[27] M. Prakash, M. Prakash, J. M. Lattimer, and C. J. Pethick, Astrophys. J. Lett. **390**, 77 (1992).

[28] B. L. Friman and O. V. Maxwell, Astrophys. J. **232**, 541 (1979).

[29] T. Takatsuka, R. Tamagaki, and T. Tatsumi, Prog. Theor. Phys. Suppl. **112**, 67 (1993).

[30] T. Muto, R. Tamagaki, and T. Tatsumi, Prog. Theor. Phys. Suppl. **112**, 159 (1993).

[31] T. Muto and T. Tatsumi, Prog. Theor. Phys. **80**, 28 (1988).

[32] A. B. Migdal, E. E. Saperstein, M. A. Troitsky, and D. N. Voskresensky, Phys. Rep. **192**, 179 (1990).

[33] M. Srednicki, Nucl. Phys. **B260**, 689 (1985).

[34] D. Kaplan, Nucl. Phys. **B260**, 215 (1985).

[35] Raffelt [15], Eq. (10.8).

[36] G. Raffelt and D. Seckel, Phys. Rev. Lett. **67**, 2605 (1991).

[37] D. K. Campbell, R. F. Dashen, and J. T. Manassah, Phys. Rev. D **12**, 979 (1975); **12**, 1010 (1975).

[38] D. B. Kaplan and A. E. Nelson, Phys. Lett. B **175**, 57 (1986).

[39] T. Muto and T. Tatsumi, Phys. Lett. B **283**, 165 (1992).

[40] H. Fujii, T. Muto, T. Tatsumi, and R. Tamagaki, Nucl. Phys. **A571**, 758 (1994); Phys. Rev. C (to be published).

[41] T. Muto, Prog. Theor. Phys. **89**, 415 (1993).

[42] A. E. Nelson, Phys. Lett. B **221**, 60 (1989).

[43] Strictly speaking, one should be comparing the axion bremsstrahlung by a nucleon in the presence of a neutral-pion condensate with the neutrino pair bremsstrahlung via nucleon-nucleon collisions in the absence of a pion condensate. In ordinary neutron-star matter, the difference in magnitude of the energy-loss rates between the neutrino pair bremsstrahlung via nucleon-nucleon collisions and the modified Urca process is relatively minor, since a lepton pair is emitted in both processes. The energy-loss rate of the latter is *only* about 16 times that of the former. Here, we used Eqs. (66a)–(66c) of Ref. [28] at $\rho = \rho_0$ with the exchange corrections properly included.

[44] There are exceptions to this rule. The simple β-decay reactions (*the direct Urca process*) are kinematically allowed in ordinary neutron-star matter either when the proton fraction is sufficiently large (Ref. [25]) or when the hyperons or nucleon isobars β decay (Ref. [27]).

[45] It is to be noted that, in contrast with the simple β decay process, this process is prohibited purely for kinematical reasons, with the composition of the neutron-star matter playing no role.

[46] S. Tsuruta, Phys. Rep. **56**, 237 (1979).

[47] According to Fig. 7 of Nomoto and Tsuruta [10], $10^2 < T/T_e < 10^3$ for the temperature in the range $T_e \sim 10^6$ K ($T \sim 10^8$ K)–$T_e \sim 10^7$ K ($T \sim 10^9$ K) for a 1.4 $M_\odot$ neutron star with the *PS* equation of state constructed by V. R. Pandharipande and R. A. Smith [Nucl. Phys. **A237**, 507 (1975)].

[48] One can make a rough estimate on the relation between the internal temperature T and the blackbody effective temperature of the surface T_e when the photon radiation from the surface dominates and the cooling reaches the quasistationary state. Let us assume that the liquid interior and the surface have uniform temperatures T and T_e, respectively, which are separated by a crust of thickness l. Heat conduction in the crust is described by the equation $q = -\kappa \nabla T$, where q is the heat current density and κ the thermal conductivity. By equating the heat conduction rate from the interior to the surface and the energy-loss rate from the surface via blackbody radiation, one finds $\Delta T = l\sigma T_e^4/\kappa$, where $\Delta T \equiv |T - T_e|$.

[49] M. S. Turner, Phys. Rev. D **45**, 1066 (1992).

[50] S. S. Murray, G. Fabbiano, A. C. Fabian, A. Epstein, and R. Giacconi, Astrophys. J. Lett. **234**, L69 (1979).

[51] B. Aschenbach, Spac. Sci. Rev. **40**, 447 (1985).

[52] P. Gorenstein, F. Seward, and W. Tucker, in *Supernova Remnants and Their X-Ray Emission: Proceedings of the IAU Symposium No. 101*, Venice, Italy, 1982, edited by J. Danziger and P. Gorenstein (Reidel, Dordrecht, The Netherlands, 1983), p. 1.

[53] J. P. Pye, K. A. Pounds, D. P. Rolf, F. D. Seward, A. Smith, and R. Willingale, Mon. Not. R. Astron. Soc. **194**, 569 (1981).

[54] T. Tatsumi, Prog. Theor. Phys. **68**, 1231 (1982).